ELSEVIER

Carbohydrate Research 337 (2002) 1467–1475

CARBOHYDRATE RESEARCH

www.elsevier.com/locate/carres

Structural features of non-granular spherulitic maize starch

Tor S. Nordmark, Gregory R. Ziegler*

Department of Food Science and Materials Research Institute, The Pennsylvania State University, 116 Borland Laboratory, University Park, PA 16802, USA

Received 11 December 2001; accepted 13 June 2002

Abstract

Complementary analyses of the internal structure of spherulites crystallized from high-amylose maize starch were obtained using light, electron and atomic force microscopy. Radially oriented crystalline lamellae were observed in transmission and scanning electron microscopy, as well as AFM. Internal structures consistent with the central hilum region of starch granules were observed. Spherulites were composed largely of linear or lightly branched starch polymers. Degradation of amylopectin at gelatinization temperatures of 180 °C was evident, but iodine binding suggested a high molecular weight (> 100 DP) for the spherulitic polymers.

Keywords: High-amylose maize starch; Structure; Spherulite; Granule formation; AFM

1. Introduction

Polymers crystallize from the melt or from concentrated solution most commonly in the form of spherulites.[1] Spherulites are polycrystalline aggregates that are more or less radially symmetric.[2] Organic polymer spherulites comprise of arrays of chain-folded lamellae. Amorphous material may be present between the radiating lamellae, and the extent of crystallinity may be low (< 50%).[3] The spherulite is birefringent. The most common extinction pattern that is observed is a ''Maltese'' cross, oriented with its arms parallel to the polarizer and analyzer vibration directions.

Unlike synthetic polymers for which spherulites are common, biopolymer spherulites are rarely observed. Kobayashi et al.[4] have recently described both positively and negatively birefringent spherulites of cellulose, and several others have investigated spherulites formed from low molecular weight ''amylose'' (DP 20–80).[5–10] Because of notable similarities, not the least of which is their common appearance when viewed with crossed polarizers, researchers have hypothesized that the native starch granule is a spherulite. However, there have not been any convincing reports of granule formation in vitro from either gelatinized (disordered) starch or polysaccharide mixtures.[11] Among the mysteries of starch granule synthesis is the mechanism of granule initiation,[12] and it is likely that the answer lies, in part, in physical–chemical, rather than biochemical, explanations that have not been fully pursued.

We have observed starch spherulites that resemble starch granules in incipient stages of development.[13] One phenomenon that can be employed to determine inner structure of spherulites is birefringence, which is defined as the difference between the radial and tangential refractive indices. Starch granules generally exhibit positive birefringence, since the refractive index is largest along the chain axis, which is oriented radially. Our previous results revealed a presence of predominantly negative but also positive birefringence in starch spherulites.[13] Spherulites made from dextrans can display both positive and negative birefringence.[5] Formation of spherulitic crystals having X-ray diffraction patterns of A- or B-type,[7] positive birefringence,[8] and radially oriented lamellae[9] have been observed in preparations of low-molecular-weight (DP 20–80) amylose and amylose–fatty acid complexes.

We demonstrated that spherulitic morphologies can develop from commercial and lipid-free high-amylose maize starch, pure amylose, and blends of amylose and

* Corresponding author. Tel.: +1-814-8632960; fax: +1-814-8636132

E-mail address: grz1@psu.edu (G.R. Ziegler).

0008-6215/02/$ - see front matter
PII: S0008-6215(02)00192-1

amylopectin (of native DP) during one cycle of heating to 180 °C, followed by rapid quenching. These results are in contrast to previous assumptions that the presence of lipids is essential for their formation.[10] Both spherulitic and non-spherulitic morphologies as judged by light microscopy conjoined with polarized light microscopy could be obtained by altering polymer composition and thermal regime.[13] Inclusion of a holding period at 95 °C in the cooling ramp provided evidence by differential scanning calorimetry for the occurrence of micro-phase separation of polymer components and lipids (when present). However, thermal degradation of the starch polymers upon heating to 180 °C was apparent during thermal analysis by differential scanning calorimtery. Thermal analysis suggested amylopectin was more heat labile than amylose, but the extent of degradation was not quantified.[13]

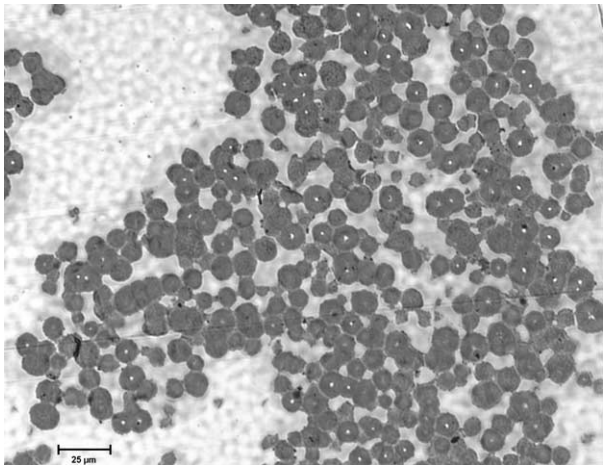

Fig. 1. Morphology of spherulites made from 10% (w/w) *ae* 70 high-amylose maize starch and embedded in a thick section cut from a block of Spurr's resin. Light microscopy (scale bar 25 µm).

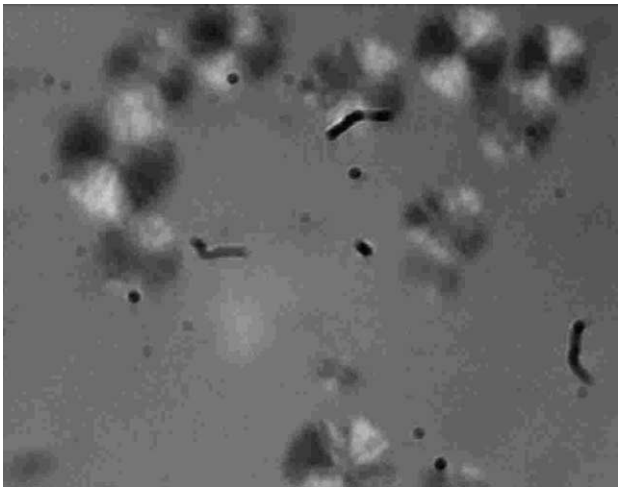

Fig. 2. Spherulites produced from 10% (w/w) *ae* 70 high-amylose maize starch embedded in a thick section cut from a block of Nanoplast resin. Polarized light microscopy (image size 53 × 68 µm). The dark fibers and dots are contaminants in the optical system.

Morphological information about starch similar and complementary to that obtained from light and electron microscopy, but without the need for staining or gold coating, can be obtained using atomic force microscopy (AFM).[14–16] AFM can provide three-dimensional surface micrographs with a resolution in nanometers, and simultaneously probe fundamental local nano-mechanical properties such as elasticity and adhesion. We chose to use AFM in tapping mode, meaning that the probe tip has an intermittent contact with the sample surface. The cantilever to which the tip is attached is oscillated at or near the cantilever's resonant frequency. The oscillation is monitored by a photodetector in connection with a laser light beam reflected from the cantilever. A feedback loop ensures that the amplitude is kept constant, and the force required is used to identify surface features.

The molecular weight and branching characteristics of the starch chains can reasonably be assumed to differ between crystalline and amorphous regions in spherulites, and between the chains in spherulitic and non-spherulitic starch. Since spherulites form more readily the higher the amylose content,[13] we hypothesized that the crystalline lamellae would be composed primarily of linear or lightly branched starch and that the highly branched amylopectin will either be trapped in interlamellar regions or excluded from the spherulite altogether. Therefore, we employed size-exclusion chromatography to investigate the composition of the spherulites.

This study was performed to determine the inner organization of high-amylose maize starch spherulites, particularly the fiber orientation and the distribution of amylose and amylopectin chains. The results are relevant to understanding of starch granule initiation and mechanisms of starch retrogradation.

2. Results and discussion

Light and polarized light microscopy.—Embedding procedures appear to have had no influence on the size of the spherulites, since the maximum diameters on the images (Figs. 1 and 2) match previous results from LM and SEM of unembedded spherulites.[13] The size distribution resulting from a nearly simultaneous and quiescent crystallization is narrow and, thus, the dimensions observed in the thick sections are mainly related to the location of the sections relative to the center of the spherulite. Spherulites in thick sections show a Maltese cross when viewed between crossed polarizers (Fig. 2). Non-median sections reveal less distinct crosses as would be expected if the spherulite were cut some

distance from the center. Therefore, we concluded that the embedding procedures have not introduced artifacts with regard to dimensions or radial inner structure.

Note the bright spots or "holes" present in the center of some sections in Fig. 1. This differential staining implies a difference in structure (density) or composition in this central region. Spherulites are thought to evolve from sheaf-like or bowtie-shaped precursors that eventually reach a radial span of dimension R beyond which growth progresses in spherically symmetric fashion (see fig. 55 in Ref. 1). The radial span R of this low-density central region increases with crystallization temperature. The presence of a hole can be used to judge if the spherulite has been sectioned radially through the center.

Electron microscopy.—Radial orientation of crystalline lamellae or "fibers" was visible in electron micrographs (Fig. 3), especially near the outer surface and the central hole. Assuming these "fibers" are composed of chain-folded lamella, consistent with synthetic polymer spherulites, this would confirm the negative birefringence reported earlier.[13] It was not unusual to see spherulites grown together. Intercrystalline links have often been observed bridging lateral faces within a single spherulite or at the boundaries between spherulites.[1]

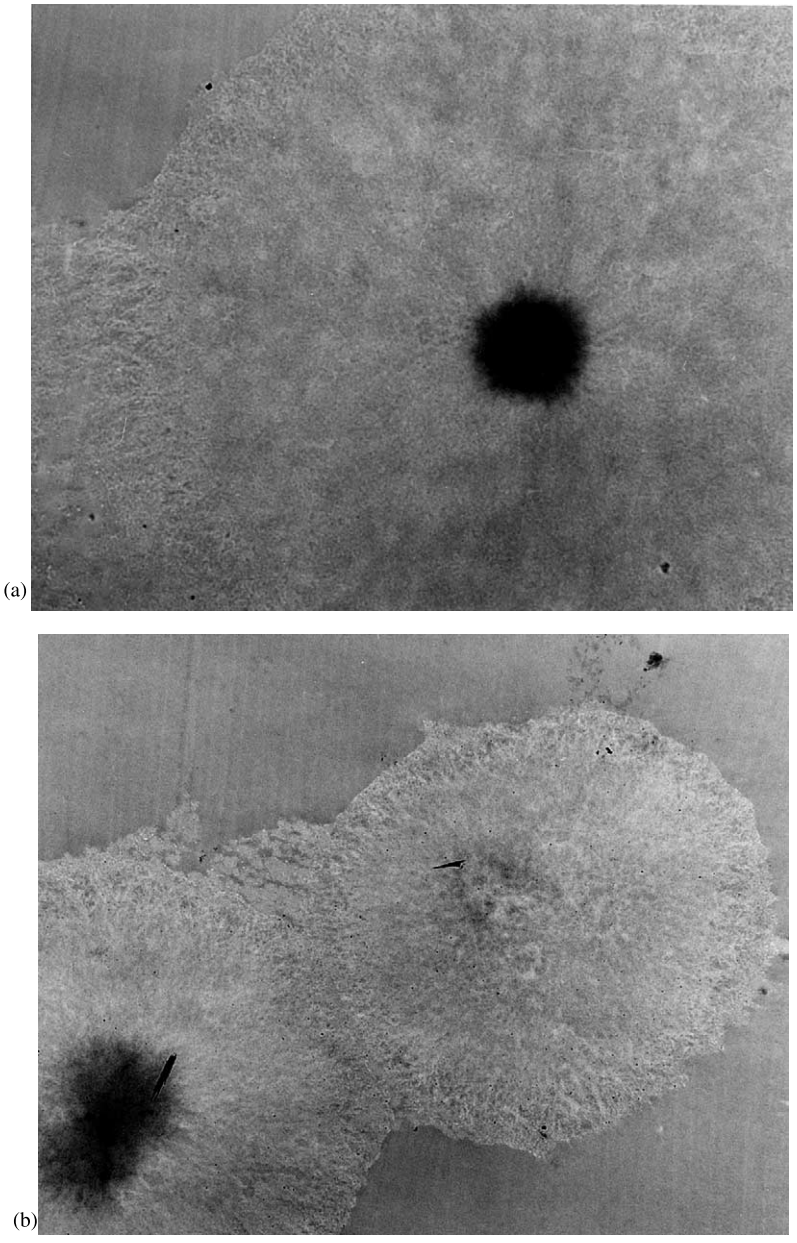

Fig. 3. Transmission electron micrographs showing radial spherulitic inner structure (from 10% w/w *ae* 70 high-amylose maize starch stained with osmium tetroxide). Embedded in Spurr's resin. (a) Image size 9.5 × 12 μm; (b) image size 11 × 14 μm.

The accumulation of the osmium tetroxide stain in the central hole is reminiscent of the anomalous "blue staining cores" observed in maize starches.[17] This central hole measures 1–3 μm, consistent with the dimensions of holes previously reported in several starch varieties.[18] Hoseney[19] identified similar features with the "hilum" or the point from which the starch granule grew. The appearance of the central hole of the spherulite would vary depending on the orientation of the section, i.e., edge-on or flat-on respective to the sheaf-like hedrite from which the spherulite grew (see fig. 56 in Ref. 1). Viewed flat-on, the hole would appear circular (Fig. 3(a)), but when viewed edge-on the hole would appear irregular (Fig. 3(b)).

Baldwin et al.[18] demonstrated the existence of spherical holes, the majority of which were 1–10 μm in diameter, located at the center of the Maltese cross in a range of starch types. They concluded that these holes originated as a result of internal stresses created within the granule on drying, but could not rule out the possibility that drying simply made the holes visible. Interestingly, holes were only visible in the small, spherical B-type wheat granules and not the lenticular A-type granules.[18] Lenticular granules form from an initial spherical core (quite similar to the B-type) upon which additional starch is deposited.[20] The B-type granules are very similar to the starch spherulites described here and could be incipient granules.

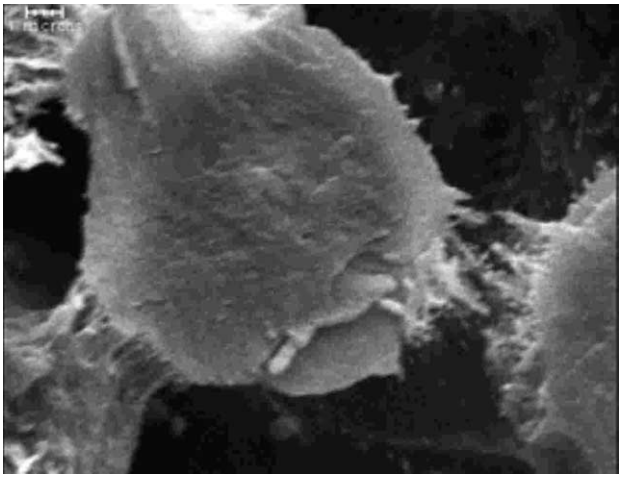

Fig. 4. Scanning electron micrograph of thermally fractured spherulites of *ae* 70 high-amylose maize starch. Bar equals 1 μm.

Cryo-fractured spherulites seemed to confirm the radial orientation of the crystalline "fibers" in the region of inter-spherulitic links (Fig. 4). No central hole is present, indicating that this fracture plane was not centrally located. The thickness of the "fibers" appears to be on the order of 100–150 nm. The typical dimension for lamellar thickness in synthetic polymer spherulites is a few hundred angstroms.[1] However, orientation is important, as the crystalline lamellae making up spherulites are thought to be ribbon-like and therefore asymmetric.

Atomic force microscopy.—Atomic force microscopy was used to probe the internal structure of starch spherulites (Fig. 5). The outer diameter and the presence of the central hole are consistent with results from light and electron microscopy. Height images consistently revealed bowtie-shaped, sheaf-like structures roughly symmetrical about the central hole (Fig. 5(a)). This sheaf-like structure is displayed by synthetic spherulites.[21] In synthetic spherulites the bright and dark areas have been identified as flat-on and edge-on lamellar regions, respectively.[3] The fine structure of starch granules has previously been investigated using AFM.[22,23]

Topological (height) and phase (modulus) images in Figs. 5(a,b) and 6(a,b) were acquired simultaneously in light tapping mode. This optimized the contrast for the topological (height) images (Figs. 5(a) and 6(a)), but would not be optimal for resolution of crystalline and amorphous regions in the phase images. Crystalline regions, with their greater Young's modulus, could be

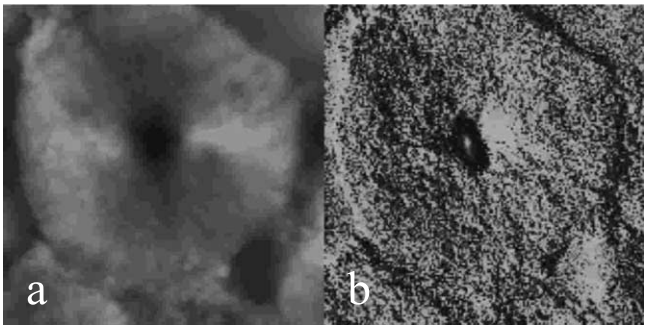

Fig. 5. Atomic force micrograph of a spherulite obtained from 10% (w/w) *ae* 70 high-amylose maize starch embedded in a thick section of Spurr's resin. Image size is 10×10 μm, height (a) and phase angle shift (b) image scales are 304 nm and 22.4°, respectively.

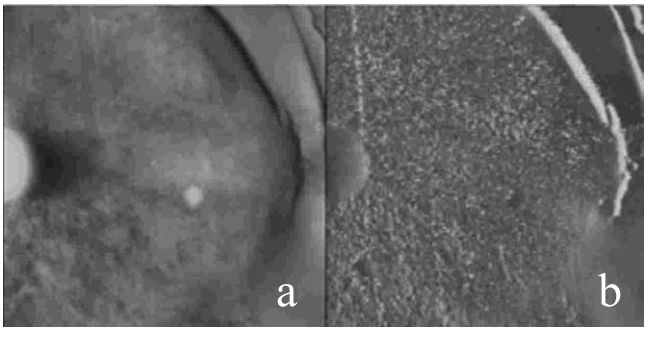

Fig. 6. Atomic force micrograph of a spherulite segment obtained from 10% (w/w) *ae* 70 high-amylose maize starch embedded in a thick section of Spurr's resin. Image size is 9.2×9.2 μm, height (a) and phase angle shift (b) scales are 151 nm and 40°, respectively.

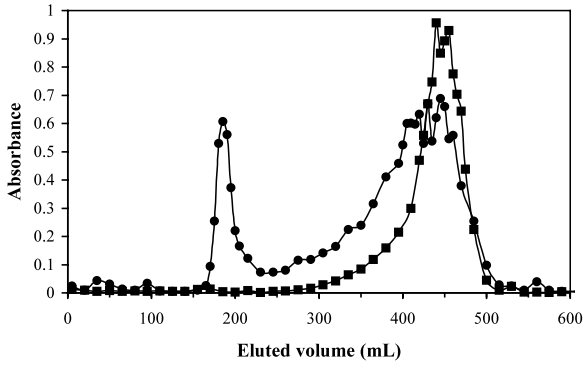

Fig. 7. Size-exclusion chromatograms of dispersed-dried *ae* 70 high-amylose maize starch (circles) and dispersed-dried spherulitic *ae* 70 high-amylose maize starch (squares) made by three-cycle heat treatment between 10 and 180 °C.

expected to appear brighter in phase contrast images (Fig. 5(b)) vis-à-vis amorphous regions.[3] A broad bright area can be seen to the right of the central hole in Fig. 5(b), possibly corresponding to a flat-on lamella face, which would be consistent with the bright area in the topological image (Fig. 5(a)). The bright spot in the center of Fig. 5(b) suggests that the central core is not empty, but contains crystalline regions, possibly an edge-on view of the original hedrite from which the spherulite grew.[1]

Fig. 6 is a slightly magnified view of another spherulite that more clearly demonstrates the radial orientation of the lamellae edges (lower left of Fig. 6(a and b)) in comparison to the flat-on face (center of Fig. 6(a and b)). Also observed in Fig. 6 were several smaller "holes" away from the center, the origin and significance of which is unknown. However, Manning and Dimick[24] have shown similar features in spherulitic cocoa butter crystals resulting from the incorporation of smaller, separately nucleated spherulites into the growing crystal mass.

Size-exclusion chromatography and DSC of heat-treated starches.—Size-exclusion chromatograms of the DDS–HAS preparation and heat-treated spherulitic HAS are shown in Fig. 7. Only traces of amylopectin and small amounts of "intermediate material" are present in the latter case, suggesting that such material is partially hydrolyzed during the three heating cycles used for the making of spherulitic starch. The washed spherulites yielded the same result (not shown) except that the amount of intermediate material was lower. In order to test the hypothesis that the amylopectin was thermally degraded during the heating cycles, waxy maize was subjected to chromatography. Degradation was evident in the heat-treated waxy maize, consistent with the pronounced sensitivity of amylopectin to high temperatures found by Vesterinen et al.[16]

The wavelength of maximum absorbance of the amylose–iodine complex in the range 410–650 nm is a non-linear function of the degree of polymerization of the starch chain, and can be used to estimate the DP up to about 100.[25–29] At DP 10–15 virtually no iodine is bound, and the color is a faint orange. A critical chain length of DP ~ 100 is required for stabilization of the ordered helix and formation of a blue complex.[25] Banks and Greenwood[25] have suggested Eq. (1):

$$\mathrm{DP}_n = 0.0096/(1/\lambda_{\max} - 0.00156) \quad (1)$$

Heat-treated *ae* 70 HAS demonstrated a $\lambda_{\max}$ of 603, regardless of the number of heat-quench cycles, corresponding to a DP of 98. The $\lambda_{\max}$ (607 nm) of heat-treated amylose was identical to that of the boiled *ae* 70 HAS, with a calculated DP of 110. $\lambda_{\max}$ for gelatinized waxy maize starch was 541 corresponding to an average DP of 33. Baba et al.[26] reported that $\lambda_{\max}$ of an amylomaize–iodine complex at 0.002% starch concentration was 602 nm. Banks and Greenwood[25] reported a $\lambda_{\max}$ of 600 nm for ordinary starch when the molarity of KI was 0.03 M (which is similar to our concentration). It is doubtful whether quantitative information about the chain lengths can be reliably obtained above DP ~ 100. However, we can conclude that, despite some thermal degradation, the starch polymers forming spherulites in this instance are significantly larger than those observed previously.[5–8]

We reported[13] that spherulites were observed using polarized light microscopy (PLM) in preparations of pure amylopectin that had been heated to 180 °C and then quenched. Samples of waxy maize starch treated with one heat cycle and then either immediately scanned in the DSC or stored for 1 day and then scanned revealed the presence of an endotherm between 80 and 90 °C, i.e., about 10 °C below the melting range of *ae* 70 spherulites. This is consistent with the melting of spherulites formed from degradation products of amylopectin. Therefore, thermal degradation products may be responsible for the appearance of spherulites in heated amylopectin.[13]

Conclusions.—Spherulites made from *ae* 70 high-amylose maize starch have been demonstrated to display a consistent size using light, electron, and atomic force microscopy. The retained birefringence with crisp Maltese crosses, even after embedding, allowed investigation of the internal structure. Spherulites appear to consist of radially oriented "fibers" that, if composed of chain-folded lamellae, double helices, or single helices with inclusion complexes with their main chain axis perpendicular to the lamella surface, would result in the negative birefringence previously reported.[13] It cannot be ruled out that the B-type X-ray diffraction pattern observed in spherulitic starch[13] resulted from secondary crystallization (retrogradation) of inter-lamellar material. We conclude that a central cavity may develop early in both spherulites and native starch granules and that their hilum regions may share a similar history of development.

3. Experimental

Materials.—Granular high-amylose (*ae* 70) maize starch (Hylon VII) and waxy maize starch (Amioca) were obtained from National Starch and Chemical Company (Bridgewater, NJ). Water was treated in a NANOpure water purification system (Barnstead/Thermolyne, Inc. Dubuque, IO) equipped with a 0.2-μm filter. Sodium hydroxide (ACS reagent grade), 1-butanol (certified ACS), phenol (ACS reagent grade) and Me_2SO (certified ACS) were obtained from Fisher Scientific Co. (Fair Lawn, NJ). Sulfuric acid (ACS reagent grade), and sodium azide were obtained from Sigma Chemical Co. (St. Louis, MO). Ethanol (USP) and acetone (ACS reagent grade) were obtained from Mallinckrodt Baker, Inc. (Paris, KY).

Preparation of spherulitic starch.—Spherulitic starch was prepared in sealed, 60-μL stainless-steel DSC pans by cyclic heating and cooling of a 10% (w/w) aqueous suspension of starch that had been stored for 1 day at ambient temperature to facilitate moisture equilibration. A DSC-7 operated with PYRIS software for WINDOWS v3.52 (Perkin–Elmer Instruments, Norwalk, CT) was used for thermal treatments. The thermal treatment started with heating from 10 to 180 °C at 10 °C/min, followed by cooling at 150 °C/min to 10 °C, heating at 10 °C/min to 95 °C, holding for 1 hour, heating at 20 °C/min to 180 °C, cooling at 150 °C/min to 10 °C, heating at 10 °C/min to 180 °C and finally cooling at 150 °C/min to 10 °C. This three-cycle procedure was judged by light microscopy to yield good contrast and crisp images of spherulites that generally did not impinge upon each other. Aqueous suspensions of 3% (w/w) granular *ae* 70 HAS starch become a homogeneous mix at 150 °C, and amylose and amylopectin are phase separated at 160 °C at the length scale of light microscopy.[16] Therefore, residual granular order should be eliminated during the thermal treatment imposed here. The issue of thermal and oxidative degradation has been addressed[16,30–32] and from this evidence we estimated the loss in amylose molecular weight due to thermal cycling to be in the range of 10–40%. The thermal sterilization of the samples in sealed pans ensured freedom from microbial activity, but would not prevent secondary crystallization from occurring over a long storage period at 4 °C.

Light and electron microscopy.—Spurr's resin[33] and Nanoplast[34,35] were employed as polymeric resins for the embedding of samples. Spurr's resin is an epoxy plastic and was made using an accelerator in a quantity commensurate with firm grade. Nanoplast is a melamine–formaldehyde plastic and was made using an accelerator in a quantity commensurate with medium grade. These resins were made on-site using kits purchased from Electron Microscopy Sciences (Fort Washington, PA) and SPI Supplies (West Chester, PA), respectively. Resin blocks were manufactured per the directions of the manufacturer with minor modifications. The samples were stained with either osmium tetroxide or uranyl acetate prior to embedding in Spurr's resin and Nanoplast, respectively. In the latter case, and prior to this staining, the samples were treated with 2.2 N HCl (which did not influence the spherulitic morphology as it appeared in LM and PLM) and then iodine to enhance the contrast in visible light for sectioning. The staining effect of iodine (0.02% I_2/0.4% KI) was weaker than expected, given the high amylose content. Resin blocks were formed in BEEM flat embedding molds from Ted Pella (Redding, CA) or SPI Supplies (West Chester, PA).

Thick sections were cut using an Ultracut UCT ultramicrotome (Leica Microsystems Inc., Deerfield, IL) equipped with a glass knife, then stained with 1% toluidine blue in 1% aq sodium borate, and baked at 50 °C (Spurr's resin) or at 100–110 °C (Nanoplast) for 15–30 s until the stain started to dehydrate. The section thickness (200–500 nm) was estimated from the interference color as the section floated on the knife trough and from the setting on the ultramicrotome. Samples were observed using a light microscope (Olympus BX 50, Olympus America, Melville, NJ, equipped with a RT Slider Spot Digital Camera Model 2.3.1, Diagnostic Instruments Inc., Sterling Heights, MI, or Nikon Diaphot 300, Nikon Inc., Melville, NY, equipped with a liquid-cooled CCD camera of type Nu 200, Photometrics Ltd., Tucson, AZ). Some unembedded specimens were also observed directly in a light microscope after staining with toluidine blue.

Thin sections (40–70 nm) were cut using an Ultracut UCT ultramicrotome (Leica Microsystems Inc., Deerfield, IL) equipped with a diamond knife (Diatome US, Inc., Fort Washington, PA). In the case of Spurr's resin, sections were placed on support film of Formvar (Electron Microscopy Sciences, Fort Washington, PA) that had been placed on a copper grid and carbon coated in a vacuum evaporator (Model 306, Edwards, Inc., Grand Island, NY). In the case of Nanoplast, sections were placed on copper grids coated with 200-mesh Lacey carbon (SPI Supplies, West Chester, PA). Samples were then observed in a JEOL 1200EXII transmission electron microscope (JEOL, Peabody, MA) operated at 80 kV.

A JEOL JSM 5400 (JEOL, Peabody, MA) was used for scanning electron microscopy (SEM) studies. High-amylose starch (10% w/w aq *ae* 70) was subjected to the heating–cooling regime in the Materials Section, and then stored for 2 months at 5 °C. The sample was then partially dried, first during 1 h at ambient temperature and then for a short period at 45–55 °C, before being gently rubbed manually between cover slips. The sample was quenched in liquid nitrogen at −196 °C, etched (moisture removal by sublimation) at −90 °C under

high vacuum for 45 min, and sputter-coated with gold while still cold in a Cryo-SEM model C1500C (Gatan Inc., Warrendale, PA) for 15 min before being observed.

Atomic force microscopy.—Imaging was performed with a Nanoscope IIIa (Nanoscope, Santa Barbara, CA) atomic force microscope operated with NANOSCOPE III v. 4.32 r3 in light tapping mode using TESP etched silicon probes with a nominal radius of 5–10 nm, a spring constant in the range 20–100 N/m, and a resonant frequency of 2–400 kHz (Digital Instruments, Santa Barbara, CA). Scan frequencies were in the range 0.2–1.5 Hz. Samples were the pristine surfaces of either resin blocks or thick sections cut off from a block as described in the "Preparation of spherulitic starch" section. They were mounted on glass and stored in a desiccator containing satd aq disodium hydrogen phosphate. Data were recorded in a single channel or simultaneously in dual channels (height/topography and phase angle shift) and then subjected to minor image processing (flattening) and image analysis. Height images are interpreted along a grayscale (bright = high) as a vertical deviation from a fixed level. The phase angle shift $\Delta\emptyset_0$ in radians between the free and interacting cantilever can be expressed as:[36]

$$\Delta\emptyset_0 \approx \varepsilon\langle a\rangle E(Q/k)$$

where Q is the quality factor of the cantilever, $\langle a\rangle$ is the radius of a circular contact area between cantilever tip and sample surface, ε is a dimensionless constant ($1.9 < \varepsilon < 2.4$), and E is the effective modulus as shown below:

$$1/E = (1 - [\nu_1]^2)/E_1 + (1 - [\nu_2]^2)/E_2$$

where E and ν are Young's modulus and Poisson's ratio, respectively, and the indices 1 and 2 refer to the tip and sample. Since E_1 is normally much larger than E_2, $E \propto E_2$. Surface regions with a higher modulus will yield a more positive phase shift $\Delta\emptyset_0$ and be displayed brighter in a phase image. Since spherulitic starch is relatively soft, the working instrument parameters (amplitude setpoint) were first chosen to provide a reliable tracking of the surface topography so that influences from any surface adhesion or capillary forces were not allowed to hinder an accurate resolution of the structures. Only a slightly harder tapping was finally chosen to avoid expansion of the contact area.

Size-exclusion chromatography and differential scanning calorimetry.—A glass column (85 × 3.0 cm) was packed with Sepharose CL-2B gel (Supelco Chromatography Products, Bellefonte, PA), which has a separation range of 70 kD–40 MD, and was used for the fractionation by size of the molecular components of four different starch preparations; (a–d) below. The alkaline eluent (aq NaOH, pH 12, with 0.02% sodium azide) was degassed for 30 min by vacuum boiling while stirring and was always used fresh (< 1 day old). The flow rate was about 0.5 mL/min The total carbohydrate content was determined using the phenol–H_2SO_4 assay,[37] employing eluent as a blank.

One sample of 10% (w/w) aq waxy starch was treated as in (d) below and used for SEC, while another waxy sample (dry weight ~4 mg) was not dispersed in Me_2SO, but heated to 180 °C at 10 °C/min, cooled to 10 °C at 150 °C/min, stored for 1 day, and then scanned in the DSC.

The starch sample in (a) was not heat treated. The starch samples in (b)–(d) below were first heat treated in a DSC in the same manner as the samples for structural studies.

(a) Dispersed-dried high-amylose starch (*ae* 70 HAS). Granular HAS was mixed with ~20 times as much aqueous 90% Me_2SO, vortexed, and heated in boiling water with constant stirring for 3 h. This liquid was brought to 4.5 times larger volume by the addition of 95% EtOH, agitated, and centrifuged for 15 min at 6500*g* (B-20A centrifuge and model 872 rotor, International Equipment Company, Needham, MA) at a temperature of 4 °C. The supernatants were discarded, and the pellets were washed in ~15 times as much 95% EtOH and re-centrifuged as just described. This washing procedure was repeated once with 95% EtOH and once with acetone. The final pellets were dried on watch glasses at 50 °C for 24 h. The dispersed-dried starch (DDS–HAS) thus obtained was stored in a desiccator with calcium sulfate (Drierite).

(b) Dispersed-dried spherulitic HAS (post heat treatment). The contents of 5 DSC pans (dry mass ~19 mg) were mixed with 100% Me_2SO in a cone-bottom glass vial to obtain a Me_2SO concentration of 90%, heated in boiling water with constant stirring for 3 h, and cooled to 20–22 °C. This liquid was mixed in vials with 95% EtOH, agitated, centrifuged (Eppendorf Centrifuge 5415 C, Brinkmann Instruments, Inc., Westbury, NY), and washed in EtOH and acetone as described above. The final pellet was dried of acetone while being stirred with a needle until a powdery substance remained. This dispersed-dried spherulitic starch was directly liquefied by adding 1 mL of aq NaOH of pH 13 (70 °C) to the vial and vortexing. It was stored covered at 45 °C until analyzed.

(c) Washed spherulitic HAS. Paste from 10 DSC pans (dry mass ~38 mg) was mixed with 1 mL of deionized water in a vial, vortexed for 2 min, treated with ultrasound (model 1200, Branson Cleaning Equipment, Co., Shelton, CT) for 5 min, vortexed briefly again, and allowed to precipitate[38] for 5 min. The supernatant was withdrawn and dried at 100 °C, and the remaining solids were weighed. The precipitate was transferred to a

weighed cone-bottom glass vial, dried partially to obtain a pasty appearance, and its moisture content was estimated. A calculated amount of 100% Me_2SO was added to the precipitate to obtain a Me_2SO concentration of ~90%. This mix was vortexed, heated in boiling water with constant stirring for 3 h, cooled to ambient temperature, and washed in EtOH and acetone. The final pellet was then dried, liquefied, and stored as described in (b) above.

(d) Dispersed-dried heat-cycled waxy maize starch. The contents of 3 DSC pans (dry mass ~12 mg), heat treated as in 3.1 above, were mixed with 100% Me_2SO and then treated and stored as described in (b) above.

After storage for 0.5–1 day, the aqueous dispersion was centrifuged at 1600*g* for 20 min at 20–22 °C, and the supernatant was removed (washed and waxy material did not yield any gel pellet at the bottom, and other materials yielded only tiny pellets). The supernatant was dispersed in 4 mL of deionized and filtered (Nanopure) water at 50 °C, and this mix was stirred until it was applied to the column.

Iodine binding.—Samples of 10% (w/w) aq *ae* 70 HAS starch were heat treated in a DSC from 10 to 180 °C at 10 °C/min and quenched to 10 °C at 150 °C/min. One, two or three heat-quench cycles were applied. Duplicate samples of purified amylose made from *ae* 70 HAS[39] were heat cycled once in the DSC at the same conditions as above. Iodine solution was made to contain 0.02% (w/w) iodine (ACS Reagent from Sigma Chemical Co., St Louis, MO) and 0.20% (w/w) potassium iodide (certified ACS from Fisher Scientific, Pittsburgh, PA). Iodine solution (4 mL) was slowly mixed with 800 μL of initial starch suspension containing 96 μg starch, so that the final starch concentration was 0.002%. This mix was further gently stirred for 1 h at 18 °C and then stored at 5 °C for 1 day. For each sample, one 1.5-mL polystyrene cuvette was supplied with 1 mL of mix. Spectrophotometric scans of the absorbance in the region 410–650 nm, followed directly after filling the cuvettes, and the wavelength (λ_{max}) of maximum absorbance of each sample was determined. Aqueous solutions with either 0.012% (w/w) *ae* 70 HAS starch or waxy maize starch that had both been boiled for 5 min were used as controls. Pure iodine solution was used as blank.

Acknowledgements

We thank Drs Donald Thompson and Koushik Seetharaman for allowing us the use of experimental equipment. We appreciate the assistance of Ms Annette Evans in conducting the size-exclusion chromatography. We are also grateful to Ms Rosemary Walsh for assistance with electron microscopy.

References

1. Khoury, F.; Passaglia, E. The Morphology of Crystalline Synthetic Polymers. In *Treatise on Solid State Chemistry*; Hannay, N. B., Ed.; Plenum: New York, 1976; Vol. 3, pp 466–472.
2. Keith, H. D.; Padden, F. J., Jr. *J. Appl. Phys.* **1963**, *34*, 2409–2421.
3. Magonov, S. N.; Godovsky, Y. *Am. Lab.* **1999**, *April*, 52–58.
4. Kobayashi, S.; Hobson, L. J.; Sakamoto, J.; Kimura, S.; Sugiyama, J.; Imai, T; Itoh, T. *Biomacromolecules* **2000**, *1*, 168–173.
5. Ring, S. G.; Miles, M. J.; Morris, V. J.; Turner, R.; Colonna, P. *Int. J. Biol. Macromol.* **1987**, *9*, 158–160.
6. Sandstedt, R. M. *Cereal Sci. Today* **1965**, *10*, 305–314, 358–359.
7. Whittam, M. A.; Noel, T. R.; Ring, S. G. *Int. J. Biol. Macromol.* **1990**, *12*, 359–362.
8. Helbert, W.; Chanzy, H.; Planchot, V.; Buleon, A.; Colonna, P. *Int. J. Biol. Macromol.* **1993**, *15*, 183–187.
9. Godet, M. C.; Bouchet, B.; Colonna, P.; Gallant, D. J.; Buleon, A. *J. Food Sci.* **1996**, *61*, 1196–1201.
10. Davies, T.; Miller, D. C.; Procter, A. A. *Starch/Stärke* **1980**, *32*, 149–158.
11. Gidley, M. J.; Cooke, D. *Biochem. Soc. Trans.* **1991**, *19*, 551–555.
12. Smith, A. M. *Curr. Opin. Plant Biol.* **1999**, *2*, 223–229.
13. Nordmark, T. S.; Ziegler, G. R. *Carbohydr. Polym.* **2002**, *49*, 439–448.
14. Baker, A. A.; Miles, M. J.; Helbert, W. *Carbohydr. Res.* **2001**, *330*, 249–256.
15. Baldwin, P. M.; Adler, J.; Davies, M. C.; Melia, C. D. *J. Cereal Sci.* **1998**, *27*, 255–265.
16. Vesterinen, E.; Suortti, T.; Autio, K. *Cereal Chem.* **2001**, *78*, 442–446.
17. French, D. Organization of Starch Granules. In *Starch Chemistry and Technology*; Whistler, R. L.; BeMiller, J. N.; Paschall, E. F., Eds., 2nd ed.; Academic: Orlando, 1984; pp 184–242.
18. Baldwin, P. M.; Adler, J.; Davies, M. C.; Melia, C. D. *Starch/Stärke* **1994**, *46*, 341–346.
19. Hoseney, R. C. *Principles of Cereal Science and Technology*; American Association of Cereal Chemists: St. Paul, MN, 1986; p 12.
20. Czaja, A. Th. *Die Stärke* **1972**, *24*, 77–80.
21. Kroschwitz, J., Ed. *Encyclopedia of Polymer Science and Engineering*; Wiley: New York, 1987; Vol. 10, p 62.
22. Ohtani, T.; Yoshino, T.; Hagiwara, S.; Maekawa, T. *Starch/Stärke* **2000**, *52*, 150–153.
23. Ohtani, T.; Yoshino, T.; Ushiki, T.; Hagiwara, S.; Maekawa, T. *J. Electron Microsc.* **2000**, *49*, 487–489.
24. Manning, D. M.; Dimick, P. S. *Food Microstruct.* **1985**, *4*, 249–265.
25. Banks, W.; Greenwood, C. T. *Starch and its Components*; Wiley: New York, 1975.
26. Baba, T.; Arai, Y.; Yamamoto, T.; Itoh, T. *Phytochemistry* **1982**, *21*, 2291–2296.
27. Immel, S.; Lichtenthaler, F. W. *Starch/Stärke* **2000**, *52*, 1–8.
28. Manners, D. J.; Stark, J. R. *Stärke* **1974**, *26*, 78–81.
29. Murdoch, K. A. *Carbohydr. Res.* **1992**, *233*, 161–174.
30. Cowie, J. M. G.; Greenwood, C. T. *J. Chem. Soc.* **1957**, 4640–4644.
31. De Meuter, P.; Amelrijckx, J.; Rahier, H.; Van Mele, B. *J. Polym. Sci. Part B: Polym. Phys.* **1999**, *37*, 2881–2892.

32. Moates, G. K.; Noel, T. R.; Parker, R.; Ring, S. G. *Carbohydr. Res.* **1997**, *298*, 327–348.
33. Spurr, A. R. *J. Ultrastruct. Res.* **1969**, *26*, 31–43.
34. Bachhuber, K.; Frösch, D. *J. Microsc.* **1983**, *130*, 1–9.
35. Helbert, W.; Chanzy, H. *Starch/Stärke* **1996**, *48*, 185–188.
36. Magonov, S. N.; Elings, V.; Whangbo, M.-H. *Surf. Sci.* **1997**, *375*, L385–L391.
37. Dubois, M.; Gilles, K. A.; Hamilton, J. K.; Rebers, P. A.; Smith, F. *Anal. Chem.* **1956**, *28*, 350–356.
38. Sun, Li. A Study of the Enzymic Hydrolysis of Solid Forms of Starch. Ph.D. Dissertation, University of East Anglia, UK, 1993; pp 69–73.
39. Klucinec, J. D. The Composition and Physical Behavior of Selected High-Amylose Maize Starches and of Fractions Determined by Differential Alcohol Precipitation. M.S. Thesis, The Pennsylvania State University, 1997.